Supporting information

Synergistic Coupling of CuNi Alloy with CoFe LDH Heterostructure on Nickel Foam toward High-Efficiency Overall Water Splitting

Dan Wang[a], Yuan Chu[a], Youzheng Wu[b], Mengkang Zhu[a], Lin Pan[a], Ruopeng Li[b], Yukai Chen[a], Wenchang Wang[a,c], Naotoshi Mitsuzaki[d], Zhidong Chen[a] *

[a] Jiangsu Key Laboratory of Advanced Catalytic Materials and Technology, Advanced Catalysis and Green Manufacturing Collaborative Innovation Center, School of Petrochemical Engineering, Changzhou University, Changzhou, Jiangsu, 213164, China

[b] MIIT Key Laboratory of Critical Materials Technology for New Energy Conversion and Storage, School of Chemistry and Chemical Engineering, Harbin Institute of Technology, Harbin 150001, China

[c] Analysis and Testing Center, NERC Biomass of Changzhou University, Changzhou, Jiangsu, 213032, China

[d] Qualtec Co., Ltd, Osaka, 590-0906, Japan

*E-mail: zdchen@cczu.edu.cn

Experimental Section

Material characterizations

The morphologies of all samples were detected via scanning electron microscopy (SEM, JEOL-JSM 6360LA) and transmission electron microscopy (TEM, JEOL-JEM 2100 F). The lattice parameters were originated from (X-ray diffraction XRD) (Bruker D8 Advance) and high-resolution transmission electron microscopy (HRTEM). The chemical composition of the sample was examined by X-ray photoelectron spectroscopy (XPS, PHI-Vesoprobe 5000 Ш).

Electrochemical measurements

The electrochemical experiments were performed on a CHI660E electrochemical workstation equipped with a three-electrode configuration in 1.0 M KOH or 1.0 M KOH + seawater. In the three-electrode system, the graphite, the Hg/HgO electrode, and the prepared sample (1×1 cm^2) are served as the counter, reference, and working electrode, respectively. For comparison, the Pt@NF and RuO_2@NF were prepared. Specifically, 5 mg of Pt/C (or RuO_2) was dispersed in mixed solution containing 240 μL ethanol and 10 μL Nafion. The above solution was then ultrasonicated for 30 min to form a homogenous ink. Finally, 50 μL of ink was loaded on the pretreated NF to control the mass loading to be 1 mg cm^{-2}, followed by drying in vacuum.

Before the linear sweep voltammetry (LSV) test, the electrodes were activated by cyclic voltammetry (CV) with a sweep rate of 0.1 V s^{-1}. The LSV curves of OER and HER were recorded at a scan rate of 5 mV s^{-1}. All potentials were converted to a reversible hydrogen electrode (RHE) by the following formula: $E_{RHE} = E_{Hg/HgO} + 0.059\ pH + 0.098$. The electrochemical impedance spectroscopy (EIS) was measured in the frequency range of 0.01 ~ 100 kHz with an amplitude of 5 mV. The double-layer capacitance (C_{dl}) was determined by CV at various scan rates (20, 40, 60, 80, 100 and 120 mV s^{-1}) in the non-Faradaic region. The stability of the samples was performed by chronopotentiometry and the multicurrent step method. All the curves displayed in this work were corrected against the 95% iR correction.

The turnover frequency (TOF) value can be evaluated with the following equation:

$$TOF = \frac{I}{znF}$$

Here, I, F, z, and n represent the current (A), Faraday constant (96485 C mol^{-1}), the number of electrons transferred during HER (z=2) or OER (z=4), and active site density (mol) during HER or OER in 1 M KOH, respectively. Referring to previous studies (Adv. Mater. 2022, 34, 2203615), CV curves were performed in 1 M PBS electrolyte (pH = 7) with a scan rate of 50 mV s^{-1}at a potential range of –0.2 to 0.6 V vs. RHE to measure the integrated charge (Q). The number of active sites (n) can be estimated according to the following formula:

$$n = \frac{Q}{zF}$$

Here F, z and Q represent Faraday constant, the number of electrons transferred during HER (z=2) or OER (z=4), and the integrated charge from the CV curve, respectively.

DFT calculations

First-principles calculations are performed by vienna ab initio simulation package (VASP)[1-2]. The generalized gradient approximation (GGA) of Perdew-Burke-Ernzerhof (PBE) is used to describe the exchange-correlation functional[3]. To accurately describe the dispersion interactions in our simulations, the DFT-D3 method was employed[4]. The cut-off energy for the plane wave basis is set to 500 eV and a 3×3×1 Monkhorst-pack mesh is employed. All models in this work are with vacuum layers of 15 Å. The top two layers of atoms were fully relaxed (atomic position) up to 10^{-4} eV/Å force minimization and max force of 0.05 eV/ Å. The DFT+U method was used to calculate the electronic properties of Fe, Co, Ni and Cu with U of 3.3, 3.4, 3.4 and 3.4 eV[5].

[1] G. Kresse, J. Furthmüller. Efficiency of ab-initio total energy calculations for metals and semiconductors using a plane-wave basis set, Computational Materials Science, 1996, 6,15-50.

[2] G. Kresse, D. Joubert, From ultrasoft pseudopotentials to the projector augmented-wave method, Physical Review B 1999, 59, 1758-1775.

[3] J.P. Perdew, K. Burke, M. Ernzerhof, Generalized Gradient Approximation Made Simple,

Physical Review Letters, 1996, 77 (18), 3865-3868.

[4] S. Grimme, J. Antony, S. Ehrlich, and S. Krieg, A Consistent and Accurate ab Initio Parametrization of Density Functional Dispersion Correction (DFT-D) for the 94 Elements H-Pu. The Journal of Chemical Physics, 2010, 132, 154104.

[5] V. I. Anisimov, Zaanen, Andersen, Band theory and Mott insulators: Hubbard U instead of Stoner I, Physical Review. B, Condensed matter 1991, 44, 943-954.

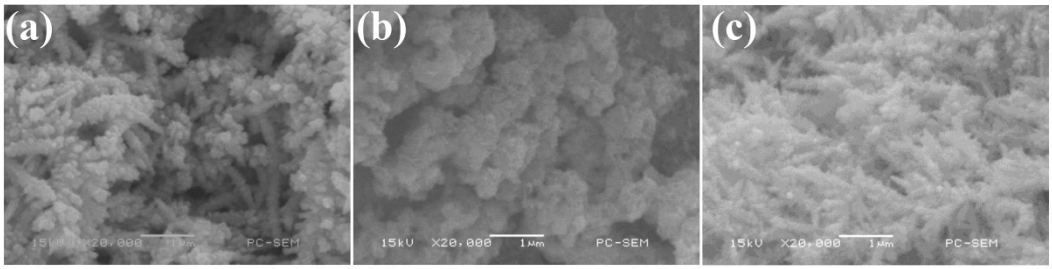

Figure S1 SEM images of (a) CuNi@NF, (b) CoFe LDH@NF, and (c) CuNi/CoFe LDH@NF.

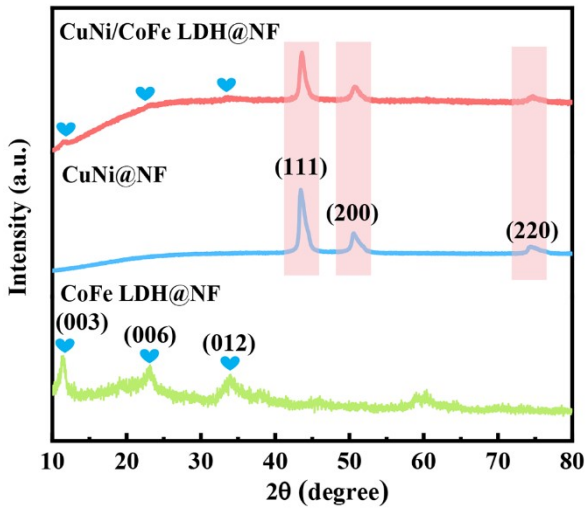

Figure S2 XRD patterns of all samples.

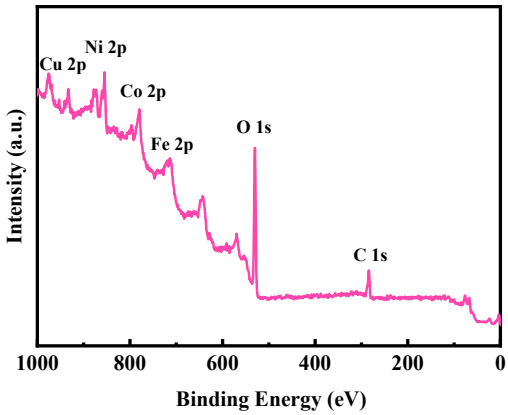

Figure S3 The overall XPS spectra of CuNi/CoFe LDH@NF.

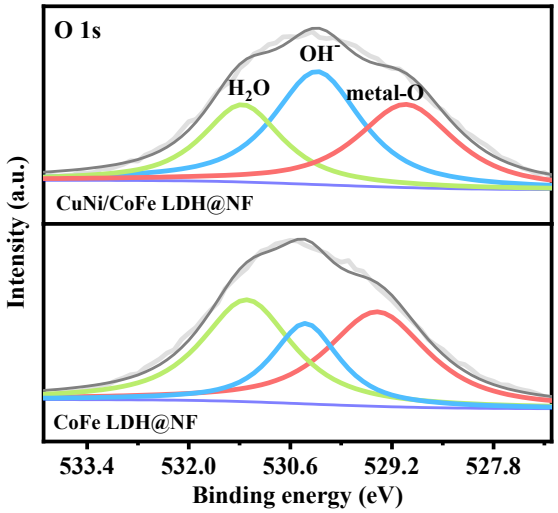

Figure S4 The O1s XPS spectra of CuNi/CoFe LDH@NF and CoFe LDH@NF.

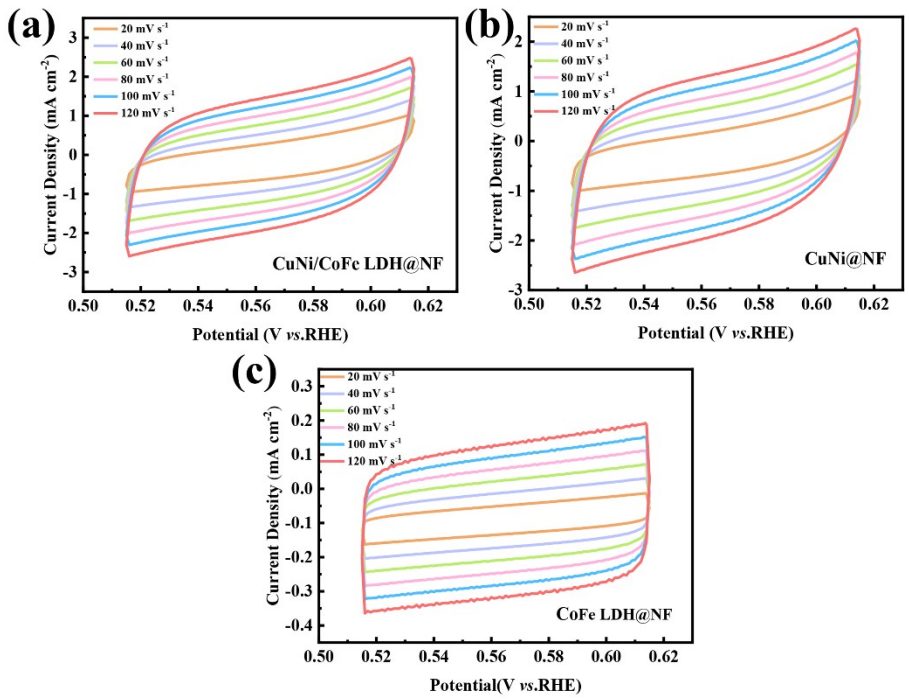

Figure S5 CV curves of (a) CuNi/CoFe LDH@NF, (b) CuNi@NF, and (c) CoFe LDH@NF in the region of 0.515~0.615 V *vs*.RHE in 1.0 M KOH at various scan rates.

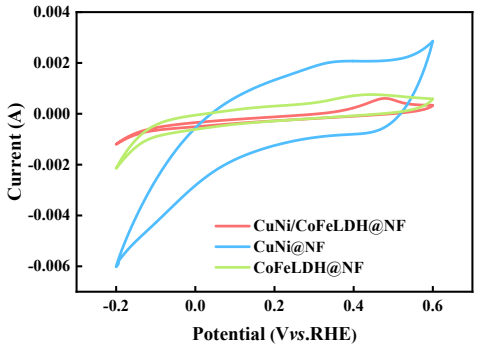

Figure S6 CVs of CuNi/CoFe LDH@NF in 1.0 M PBS (pH=7) with a scan rate of 50 mV s^{-1}.

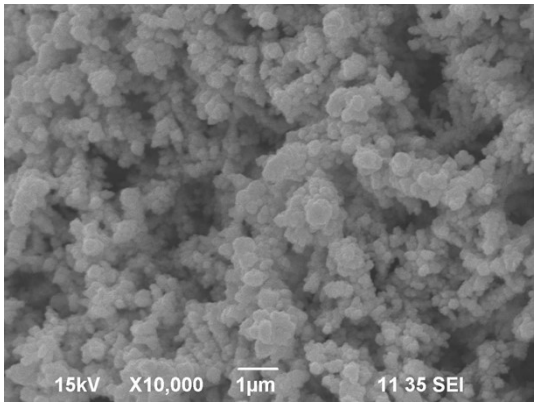

Figure S7 SEM image of CuNi/CoFe LDH@NF after HER stability test.

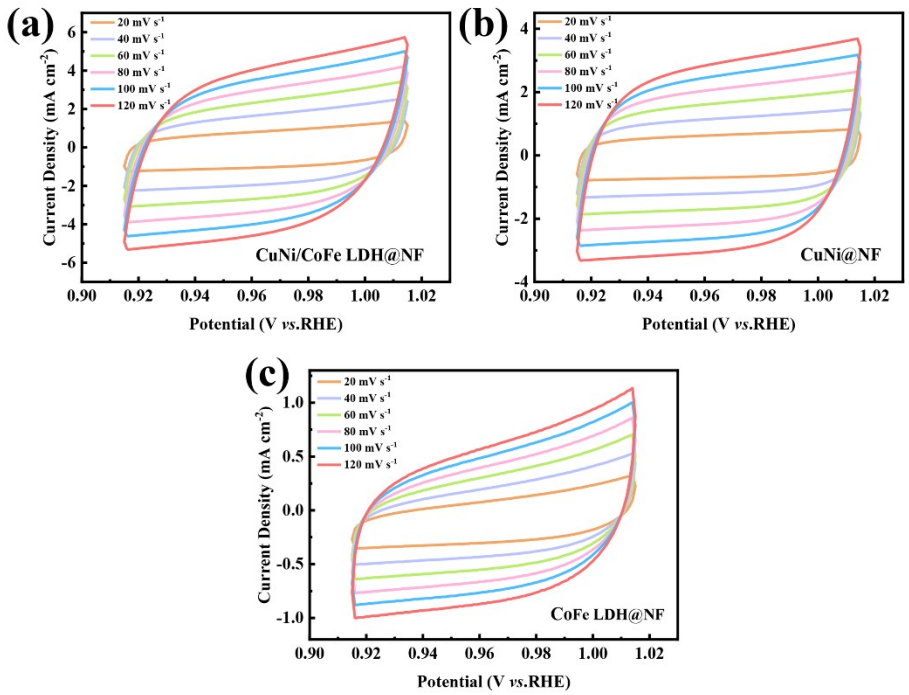

Figure S8 CV curves of (a) CuNi/CoFe LDH@NF, (b) CuNi@NF, and (c) CoFe LDH@NF in the region of 0.915~1.015 V *vs*.RHE in 1.0 M KOH at various scan rates.

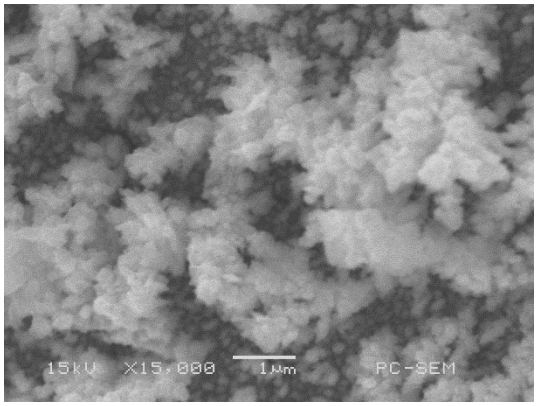

Figure S9 SEM image of CuNi/CoFe LDH@NF after OER stability test.

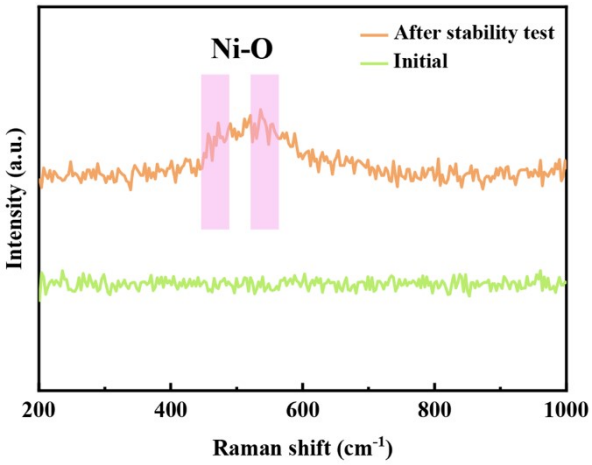

Figure S10 Raman spectra for CuNi/CoFe LDH@NF before and after stability test.

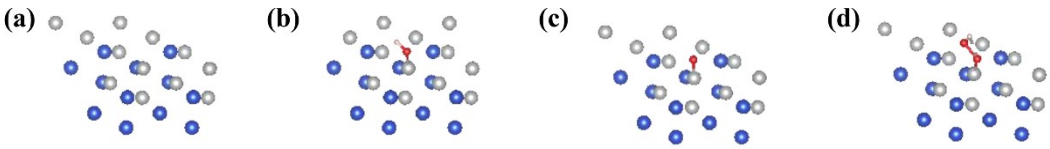

Figure S11 The absorption models of CuNi (111) and intermediates on CuNi (111). (a) CuNi (111), (b) *OH, (c) *O, (d) *OOH.

Table S1 Comparison of HER performance with those of recently reported catalysts in 1 M KOH (10 $mA \cdot cm^{-2}$).

Electrocatalysts	Overpotential (mV)	References
CuNi/CoFe LDH@NF	56	*This work*
CoP/NiCoP/NC	75	*Adv. Funct. Mater. 2019, 29 (6), 1807976*
Ni_2P-Fe_2P/NF	92	*Adv. Funct. Mater. 2021, 31 (1), 2006484*
CoP NFs	136	*ACS Catal. 2020, 10 (1), 412-419*
CoSe/$Co(OH)_2$-CM (AE)	207	*Composites, Part B 2022, 236, 109823*
FCN-8P	77	*Inorg. Chem. Front. 2024, 11, 3585*
$NiFe_2O_4$/CoNi-S	149	*Int. J. Hydrog. Energy 2021, 46 (12), 8557–8566*
FeCoMoP-O	111	*J. Alloy. Compd. 2020, 820, 153161*
$CuFe(S_{0.8}Se_{0.2})_2$	113	*Inorg. Chem. Front. 2023, 10, 2387*
MoS_2/NiFe NPs/NFL/CC	118	*Inorg. Chem. Front. 2023, 10, 1603*

Table S2 Comparison of OER performance with those of recently reported catalysts in 1 M KOH.

Electrocatalysts	Overpotential (mV)	Current density (mA cm^{-2})	References
CuNi/CoFe LDH@NF	268	50	*This work*
CuNi/CoFe LDH@NF	310	100	*This work*
Fe–Ni_2P@P-C/CuxS	330	50	*Nano Energy 2021, 84, 105861*
NiFe-LDH-Vo@NiCu	309	100	*Chem. Eng. J. 2022, 446, 137226*
NiCo-LDH-OH	317	10	*J. Colloid Interface Sci. 2023, 636,11-20*
Ni_3N–CeO_2/NF	341	50	*Adv. Funct. Mater. 2023, 33, 2306786*
CoNi-LDH/Co@NC	359	100	*Electrochim. Acta 2023, 444, 141956*
NiFeP@TiO_2-x	300	100	*J. Colloid Interface Sci. 2023, 645, 66-75*
S-CoOx/NF	370	100	*Nano Energy 2020, 71, 104652*